Bond Behaviour of Externally Bonded FRP Under Cyclic Loading

G. Ramesh, Ravindra Gettu and B. H. Bharatkumar

Abstract Strengthening of concrete structures through external bonding of fibre-reinforced polymer (FRP) composites has become a popular technique due to its advantages such as strength-to-weight and stiffness ratios, etc. In this investigation, a test method similar to RILEM TC-RC5 (used to evaluate the bond strength of rebars in concrete) is extended to evaluate bond behaviour of externally bonded FRP sheets. In the present study, experimental investigations on two types of FRP composites (with carbon and glass fibres) have been carried out, and the tensile force on the FRP versus bond–slip response has been evaluated. Both monotonic and cyclic loadings have been carried out to study the envelope response and debonding process for the chosen bond length and width. The average ultimate slip for CFRP and GFRP for selected bond length under monotonic loading was 2.28 and 2.03 mm, respectively, and in the case of cyclic loading was 1.95 and 1.76 mm, respectively. The reduction in the bond–slip under cyclic loading is due to partial debonding of FRP during repeated loading and unloading cycles.

Keywords Bond cyclic · Envelope curve · Bond–slip · Epoxy-concrete interface Debonding

1 Introduction

Externally bonded fibre-reinforced polymer (EBFRP) laminates or sheets have been used for strengthening, repair, and retrofitting for more than three decades. EBFRP sheets have benefits such as high strength-to-weight ratio, high stiffness-to-weight ratio, corrosion resistance, easy handling and can be moulded into any shape. The failure of the FRP strengthened RC flexural member is often controlled by the

G. Ramesh (✉) · B. H. Bharatkumar
CSIR-Structural Engineering Research Centre, Chennai 600113, India
e-mail: grm@serc.res.in

R. Gettu
Indian Institute of Technology, Madras, Chennai 600036, India

A. Rama Mohan Rao and K. Ramanjaneyulu (eds.), *Recent Advances in Structural Engineering, Volume 2*, Lecture Notes in Civil Engineering 12,
https://doi.org/10.1007/978-981-13-0365-4_67

debonding (peeling of the fibre) of FRP from the concrete substrate rather than by crushing of concrete or by tensile rupture of FRP [1–5]. Since the behaviour of EBFRP strengthened members depends on the bonding of FRP to concrete interface and the characteristics of the concrete substrate, it is useful to characterize the bond response adequately.

Many available test methods for the evaluation of FRP bond behaviour are based on single and double shear pull out type of tests [6–10], which do not simulate flexure. To overcome this limitation, a method similar to RILEM TC-RC5 [11–14] (used to evaluate bond strength of rebar in concrete) is used in the present investigation to evaluate the bond behaviour of EBFRP sheets. In this study, the effect of cyclic loading on bond behaviour of FRP strengthened elements has also been evaluated. The experimental results are used to compare the bond behaviour of carbon and glass fibre sheets at the FRP-concrete interface under monotonic and cyclic loading.

2 Experimental Details

2.1 Materials Used

CFRP and GFRP sheets with unidirectional fibres were used in the study along with the epoxy resin recommended by the manufacturer. The fibre properties given by the manufacturer are shown in Table 1. Steel fibre-reinforced concrete, with a characteristic compressive strength of 50 MPa, was used in this study to cast the test specimens; the steel fibres were used to prevent diagonal shear cracking of the concrete.

Before bonding the FRP to the concrete, the surface was roughened with a powered wire brush. The initial primer coat was applied over the bonded surface to fill the voids and make the surface even. The fibre sheets were saturated with the prescribed epoxy, and the saturated sheet was pressed on to the concrete surface. The pressure was applied using a ribbed roller to ensure the penetration of epoxy between the fibres.

Table 1 Properties of fibres

Data are given by the manufacturer	E-glass	Carbon
Thickness of the fibre, gsm	900	230
Modulus of elasticity, kN/mm^2	73	240
Tensile strength, N/mm^2	3400	3800
Density, g/cm^3	2.6	1.7
Ultimate strain, %	4.5	1.6

2.2 Test Details

The method proposed by RILEM TC-RC5 [7] for assessing bond characteristics of conventional steel rods was adopted with minor modifications in the size of the test specimens. The geometry, test configurations, and schematic of bonded region are shown in Fig. 1. Two separate concrete blocks, designated as A and B, are interconnected by means of a mild steel hinge arrangement located at the central portion of the specimen. At the bottom portion of the specimen, 50-mm-wide FRP composites are bonded over a length of 100 mm. The test region was always kept in block A in this investigation, whereas the FRP bonded to block B is firmly fixed to trigger the failure in the bonded region of A only. The test specimen is placed in a three-point bending frame with a load capacity of 500 kN under piston displacement control mode. The rate of loading was about 0.05 mm/min until failure.

Figure 2 shows the typical test setup. The FRP was instrumented with four strain gauges of 5 mm length at the locations referred to as S1, S2, S3, and S4 (see Fig. 3). Two linear variable differential transformers (LVDTs) with 25 mm span were used for measuring the loaded end slip. In this study, slip refers to the movement of the FRP sheet relative to the concrete. The cyclic test methodology involves two loading and two unloading cycles at each strain level. In this programme, the signal from one of the strain gauges fixed in the bonded zone was used as the controlling parameter for the loading and the reloading cycles. The specimen was loaded until the strain of SG1, the first strain gauge (i.e., nearest to the hinged face), reached a value of 1000 microstrains then unloaded. The reloading point for each unloading cycle was about 1.0 kN. Two loading and two unloading cycles were performed before continuing the loading until 2000 microstrain, when the unloading-reloading is repeated. So on, for every 1000 microstrain increment, till the subsequent strain guage SG2 reaches 1000 microstrain. When the strain of SG2, the second strain gauge, reaches the strain level of 1000 microstrains, subsequent

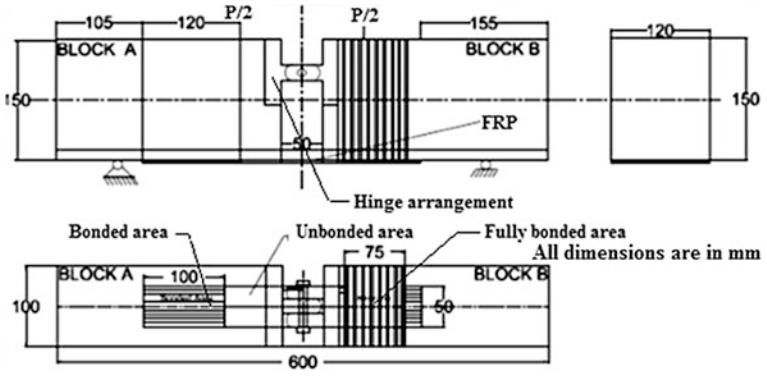

Fig. 1 Specimen geometry and test configuration of modified RILEM TC-RC-5 (1982)

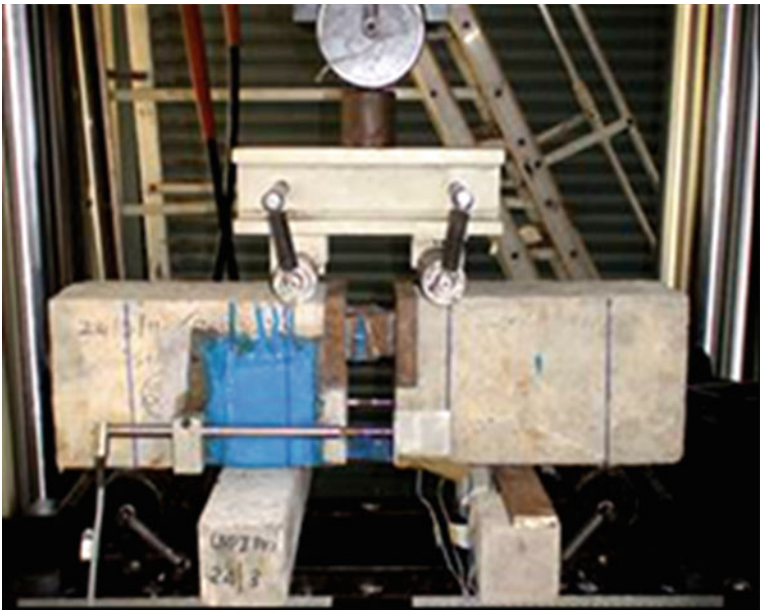

Fig. 2 Closer view of test setup

cycles were done on the basis of the strain in the second gauge. This was continued till the strains in SG3 and SG4, the third and fourth strain gauges, reached 1000 microstrains. All the sensors were monitored with a data logger.

3 Discussions of Test Results

3.1 Failure Pattern (Cyclic)

The failure in CFRP-bonded specimens in Series I (with 100 mm bond length) was by peeling and some cracking of the FRP, with debonding in the adhesive layer or in the concrete. Typical debonded specimens can be seen in Fig. 4. Failure occurred along the FRP-epoxy interface or along the concrete-epoxy interface. The CFRP-bonded specimen failed suddenly with an explosive sound, while in the GFRP-bonded specimens, the failure was progressive. The debonded surfaces are shown in Figs. 4 and 5. The failure in CFRP-bonded specimens was peeling and fracture of FRP with explosive sound, while the failure in GFRP-bonded specimen was progressive debonding.

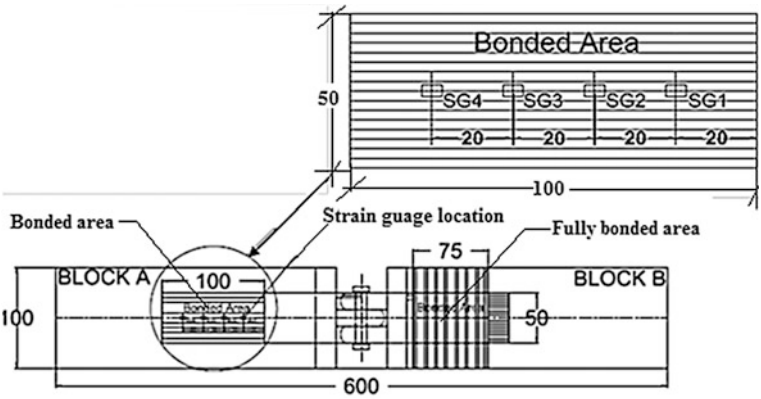

Fig. 3 Typical positioning of strain gages for 100 mm bond length and 50 mm bond width

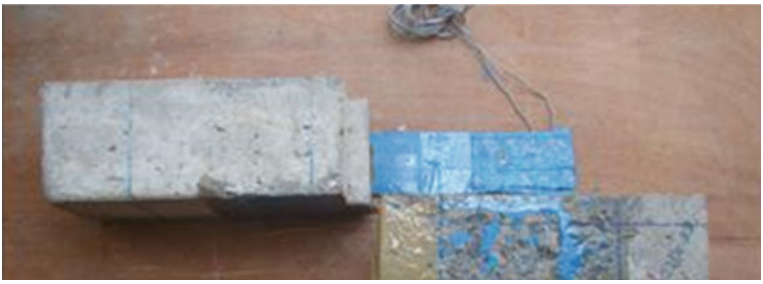

Fig. 4 Failure in CFRP-bonded specimens (50-100-C)

Fig. 5 Failure in GFRP-bonded specimens (50-100-G)

3.2 Monotonic Result Tensile Pullout Force on FRP—Bond–Slip Behaviour

Parameters such as the average maximum tensile force on fibre, peak bond shear stress or bond strength (τ_{umax}) and average ultimate deflection for each series of specimens have been obtained and reported in Table 2. Figures 6 and 7 show the load-bond–slip behaviour of the CFRP- and GFRP-bonded specimens. The average data from the two LVDTs are used to calculate the bond–slip. It was seen that the average ultimate slip was higher for carbon FRP when compared to glass FRP; the ultimate slip for CFRP is 2.28 mm and for GFRP is 2.03 mm. The average bond pullout force developed, from the three tests, for CFRP is 214 N/mm and for GFRP is 226 N/mm.

3.3 Cyclic Result Tensile Pullout Force on FRP—Bond–Slip Behaviour

Figures 8 and 9 show the evolution of the cyclic bond–slip at the loaded end and the tensile force on FRP. Parameters such as the average maximum tensile force on fibre, peak bond shear stress or bond strength (τ_{umax}) and average ultimate deflection for each series of specimens have been obtained and reported in Table 2 From the experimental bond versus slip curve, it is observed that the curve consists of three regimes. The first part is linear up to a load level of 50–60% of the maximum load attained from the specimen. The tensile force versus slip response has an initial linear regime up to about 6 kN, after which the load increases with a decreasing slope until failure occurs. Beyond that, there is some nonlinearity, at which stage debonding starts from the loaded end. Subsequently, complete debonding occurs throughout the bond length. In the final stage, sudden failure occurs. The maximum tensile force on unit width of CFRP and GFRP was 214 and 226 N/mm, respectively, under monotonic loading and was 212 and 223 N/mm, respectively, under cyclic loading. The influence of cyclic loading is not affecting the tensile forces on FRP much in both the glass and carbon fibres. The tensile force

Table 2 Parameters of experimental bond–slip loads for monotonic and cyclic loading (mean and std. deviation)

Series	Specimens	Maximum tensile force on unit width of FRP (N/mm)	Bond strength (MPa/mm)	Bond–slip, δ_f (mm)
I (mono)	50-100-C-1,2,3	214±0.02	0.042±0.02	2.28±0.22
II (mono)	50-100-G-1,2,3	226±0.81	0.045±0.16	2.03±0.46
I (cyc)	50-100-C-1,2,3	212±0.01	0.041±0.004	1.95±0.05
II (cyc)	50-100-G-1,2,3	223±0.02	0.044±0.002	1.76±0.08

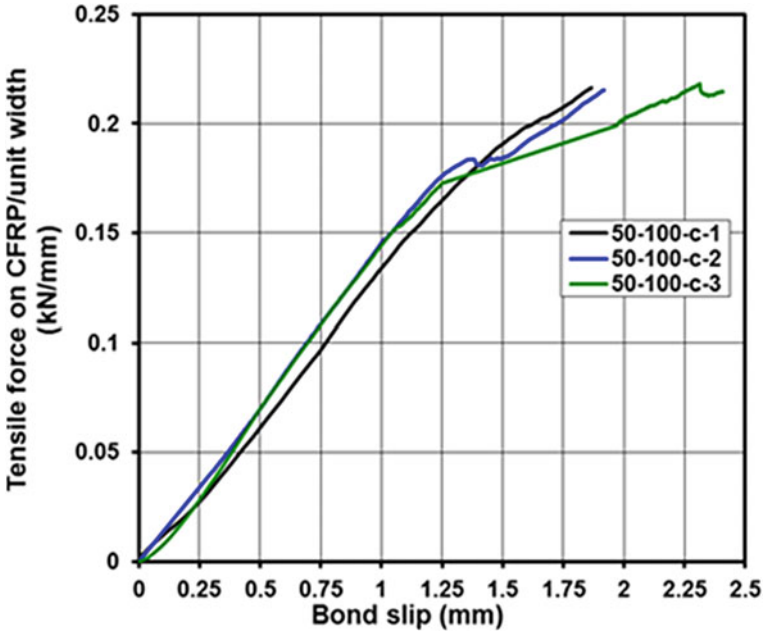

Fig. 6 Tensile force on FRP with slip in CFRP-bonded specimens

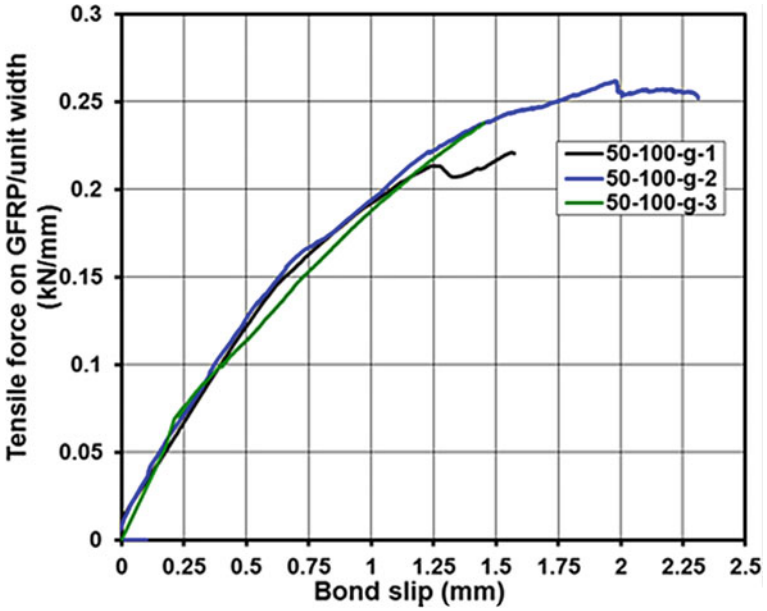

Fig. 7 Tensile force on FRP with slip in GFRP-bonded specimens

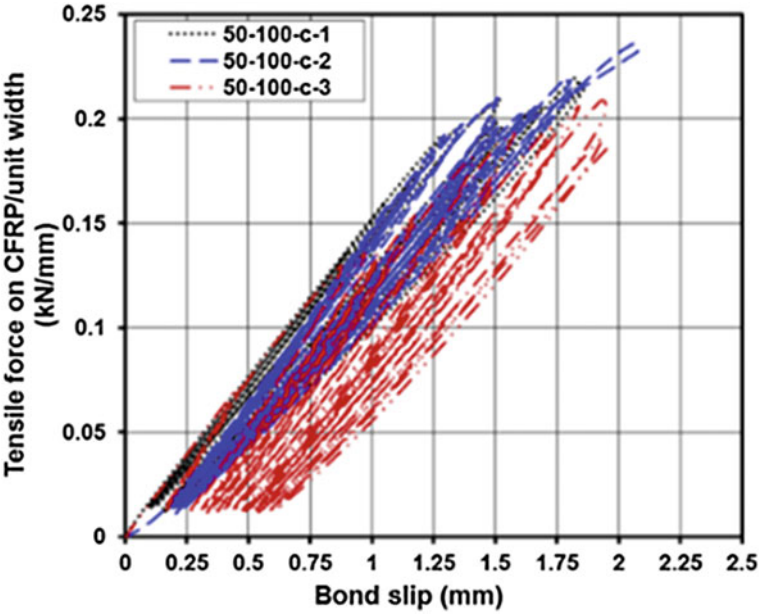

Fig. 8 Cyclic tensile force on FRP with slip in CFRP-bonded specimens

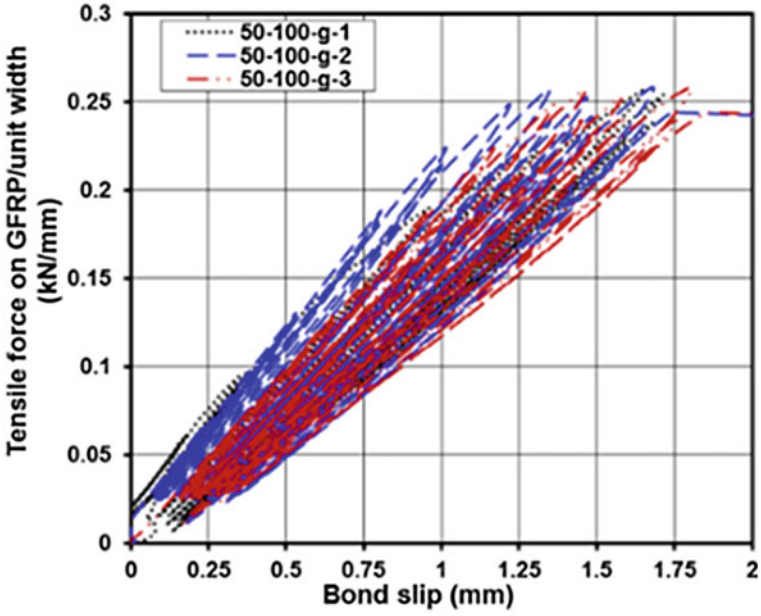

Fig. 9 Cyclic tensile force on FRP with slip in GFRP-bonded specimens

on FRP is not influenced by the type of FRP. This may be due to the fact that the bond behaviour is fully dependent on the interface between the concrete and epoxy.

The average ultimate slip for CFRP and GFRP under monotonic loading was 2.28 and 2.03 mm, respectively, and in the case of cyclic loading was 1.95 and 1.76 mm, respectively. From the experimental observations, it was found that there was a reduction in bond–slip under cyclic loading which is due to partial debonding of FRP due to repeated loading and unloading cycles. The unloading and reloading cycles in this investigation were performed in the pre-peak and post-peak regime to study the bond–stiffness degradation. Stiffness is defined as the slope of the line connecting the points corresponding to the beginning of the unloading and reloading. Bond stiffness is purely governed by friction between the bond surface (concrete), FRP fibre, and the epoxy interface. In the pre-peak region, there is no much degradation in stiffness in the both carbon and glass fibres in the unloading and reloading cycles. In the pre-peak, the number of cycles is not having any influence on debonding due to cyclic loading. The residual bond–slip in the unloading and reloading is minimal for the chosen bond length and width. After reaching the post-peak, the stiffness decreases significantly. This can be attributed to the progressive debonding of the CFRP epoxy and epoxy-concrete interfaces up to the peak force. At that stage, bond between the bond surface and FRP loses friction leads to increase in the bond–slip.

The cyclic tensile force on the fibre versus bond–slip curve traces the monotonic curve till failure in both the carbon and glass fibre. In the strain-based cyclic loading, the tensile force on FRP versus bond–slip traces the monotonic response. In the case of the CFRP-to-concrete joints, for the same cyclic behaviour, lower maximum slip values were observed for GFRP-bonded joints. Similar behaviour is observed for the monotonic specimens in GFRP. The effect of repeated loading and unloading leads to decrease in maximum ultimate slip for both the CFRP- and GFRP-bonded joints for the selected bond length and width. Similar observations were made by Ko and Sato [15] that the monotonic response envelope coincides with the cyclic curves; they also observed that plastic displacement and reduction in stiffness were observed due to partial debonding imposed by repeated unloading and reloading cycles. In terms of bond–slip GFRP, bonded specimens shows significant improvement compared to the CFRP specimens in both the cyclic and monotonic loading.

3.4 Envelope Curve

Figures 10 and 11 show the cyclic response in terms of the tensile force per unit width of FRP versus bond–slip along with the monotonic response. It can be seen that there is a close correspondence between the load envelope obtained from the monotonic tests and the cyclic response. The envelope curve of cyclic response in terms of tensile force per unit width of FRP versus bond–slip follows the monotonic response till 90% of failure load.

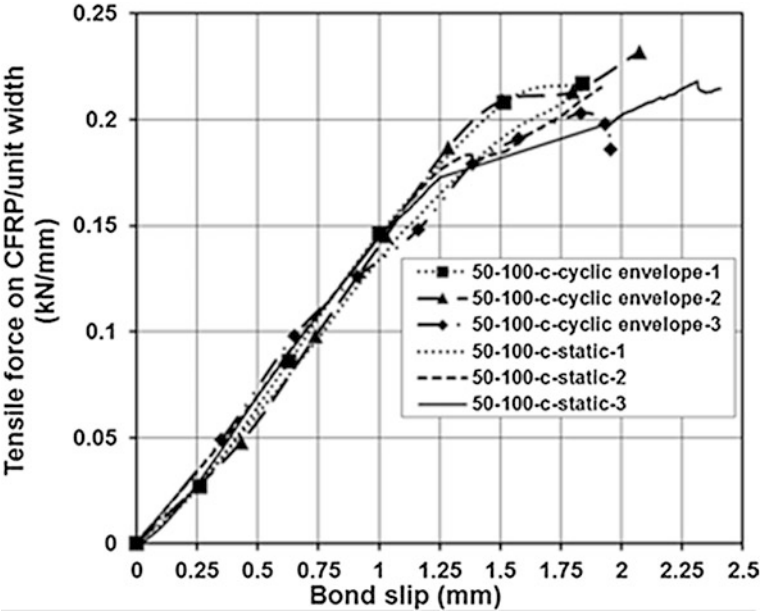

Fig. 10 Cyclic and static tensile force versus with slip in CFRP-bonded specimens

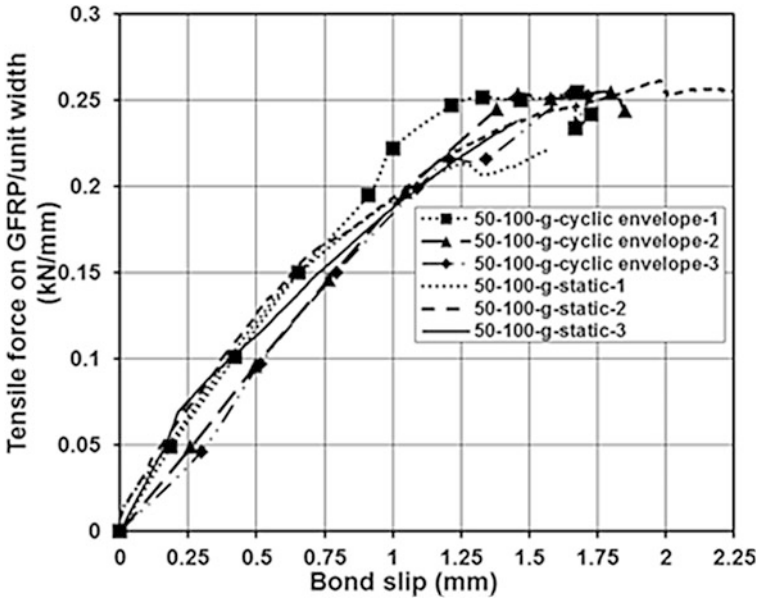

Fig. 11 Cyclic and static tensile force versus with slip in GFRP-bonded specimens

4 Cyclic Strain Distribution of CFRP- and GFRP-Bonded Specimens

Figures 12 and 13 show the tensile force on FRP per unit width versus strain plot of both CFRP- and GFRP-bonded specimens. Strain cycle and the increment of successive strains from all four strain gauges observed during first strain cycles at 1000 με interval in the first strain gauge reach about 60–70% of debonding force on FRP, and subsequent debonding of FRP sheet (50-100-C) is reported till the second strain gauge reaches the 1000 με target. Similarly, strain evolution during second strain gauge 1000 με interval cycles at 85% of debonding force and subsequent debonding for FRP sheet is reported in till the third strain gauge reaches the 1000 με interval. In the third strain gauge, 1000 με strain cycle the debonding force is 95% of the tensile force on FRP. Finally, the fourth strain gauge reaches less than 500–700 με complete debonding occurred in the FRP sheet. FRP strains are very regular showing an exponential decay starting from the loaded section. From the strain distribution, it can be seen that, at early stages of loading, the curves show linear behaviour in the loaded end. It can be assumed that bond failure begins immediately after the point when the curve becomes parabolic shape and leads to uniform distribution of bond stress along the CFRP and GFRP sheet. As expected,

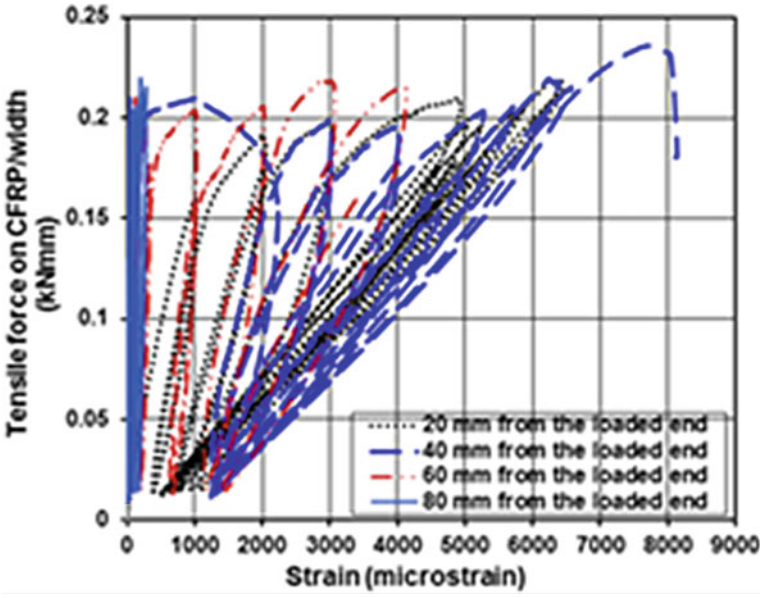

Fig. 12 Typical cyclic experimental tensile force on FRP per unit width versus strain for externally bonded CFRP specimens

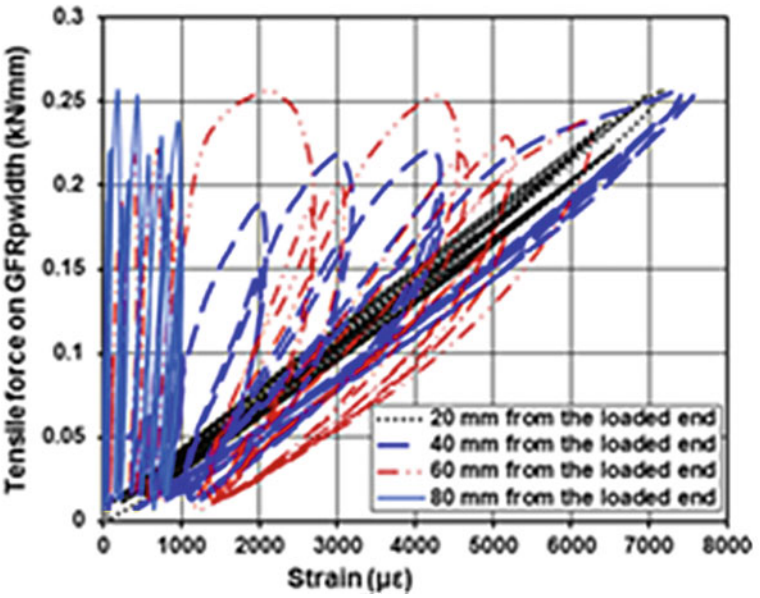

Fig. 13 Typical cyclic experimental tensile force on FRP per unit width versus strain for externally bonded GFRP specimens

the ultimate slip of CFRP sheet is higher with respect to GFRP ones, but the tensile force on FRP observed during the strain cycles is comparable with that seen under monotonic loading.

5 Conclusions

A simple beam bending test was designed for evaluation of FRP bond behaviour by modifying the RILEM TC-85 recommendation for rebar bond test. The following conclusions were drawn from the study carried out for selected bond length and width of FRP bonding under monotonic and cyclic loading:

- The failure in CFRP-bonded specimens was peeling and fracture of FRP with an explosive sound, while the failure in GFRP-bonded specimen was progressive debonding.
- The maximum tensile force on unit width of CFRP and GFRP was 214 and 226 N/mm, respectively, under monotonic loading and was 212 and 223 N/mm, respectively, under cyclic loading. The tensile force on FRP is not influenced by the type FRP. This may be due to the fact that the bond behaviour fully is dependent on the interface between the concrete and epoxy.

- The average ultimate slip for CFRP and GFRP under monotonic loading was 2.28 and 2.03 mm, respectively, and in the case of cyclic loading was 1.95 and 1.76 mm, respectively. The lower slip under cyclic loading is due to partial debonding of FRP due to repeated loading cycles.
- The envelope curve of cyclic response in term of tensile force per unit width of FRP versus bond–slip follows the monotonic response till 90% of failure load.

Acknowledgements The author acknowledges the help rendered by the technical staff of Advanced Materials Laboratory, CSIR-SERC.

References

1. Jones R, Swamy RN, Bloxham J, Bouderbalah A (1980) Composite behavior of concrete beams with epoxy bonded external reinforcement. Int J Cement Compos 2(2):91–107
2. Van Gemert DA (1980) Repairing of concrete structures by externally bonded steel plates. Int J Adhes 2:67–72
3. Oehlers DJ, Moran JP (1990) Premature failure of externally plated reinforced concrete beams. J Struct Eng 116(4):978–995
4. Quantrill RJ, Hollaway LC, Thorne AM (1996) Experimental and analytical investigation of FRP strengthened beam response: part I. Mag Concr Res 48(177):331–342
5. Triantafillou TC, Plevris N (1992) Strengthening of RC beams with epoxy-bonded fiber-composite materials. Mater Struct 25:201–211
6. Chajes MJ, Finch WW Jr, Januszka TF, Theodore Thomson A Jr (1996) Bond and force transfer of composite material plates bonded to concrete. ACI struct 93(2):209–217
7. RILEM TC-RC5 (1982) Bond test for reinforcement steel. 1. Beam test. Mater Struct 6(32):213–217
8. Yao J, Teng JG, Chen JF (2005) Experimental study on FRP-to-concrete bonded joints. J Compos Eng, Part-B 36(2):99–113
9. Brosens K, Van Gemert D (1997) Anchoring stresses between concrete and carbon fibre reinforced laminates. In: Non-metallic (FRP) reinforcement for concrete structures, vol 1. Japan Concrete Institute, pp 271–278
10. Bizindavyi L, Neale KW (1999) Transfer lengths and bond strengths for composites bonded to concrete. J Compos Constr 3–4:153–160
11. De Lorenzis L, Miller B, Nanni A (2001) Bond of FRP laminates to concrete. ACI Mater 98 (3):256–264
12. Miller B, Nanni A (1999) Bond between carbon fiber reinforced polymer sheets and concrete. In: Bank LC (ed) Proceedings ASCE 5th materials congress, New York, pp 240–247
13. Harmon TG, Kim YJ, Kardos J, Johnson T, Stark A (2003) Bond of surface-mounted fiber-reinforced polymer reinforcement for concrete structures. ACI Struct J 100(5):557–564
14. Ramos G, Casas JR, Alarcón A (2006) Normalized test for prediction of debonding failure in concrete elements strengthened with CFRP. J Compos Constr 10(6):509–519
15. Ko H, Sato Y (2007) Bond stress–slip relationship between FRP sheet and concrete under cyclic load. J Compos Constr 11(4):419–426